Supplementary Material for "Mitigating Electrochemical Degradation in Optimal Vehicle-to-Grid Dispatch via Digital Twin"

Chao Lei, *Senior Member, IEEE*, and Yu Christine Chen, *Member, IEEE*

I. Effect of SEI Thickness on Its Rate of Growth

In Fig. 1, we plot $\Delta\theta_i^{t+1}$ with respect to S_i^t and I_i^t given different values of θ_i^t. Via visual inspection, we find that the $\Delta\theta_i^t$ surfaces do not vary significantly across $\theta_i^t = 0\,\text{nm}$, $\theta_i^t = 20\,\text{nm}$, $\theta_i^t = 40\,\text{nm}$, and $\theta_i^t = 80\,\text{nm}$. This offers justification for neglecting the effects of θ_i^t in Θ in Section II-A of the main paper.

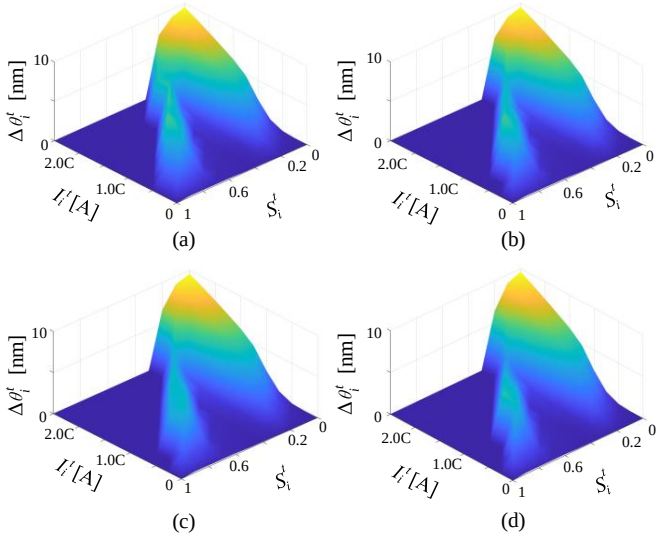

Fig. 1. PDE-based SEI growth surface $\Delta\theta_i^t$ with (a) $\theta_i^t = 0\,\text{nm}$, (b) $\theta_i^t = 20\,\text{nm}$, (c) $\theta_i^t = 40\,\text{nm}$, and (d) $\theta_i^t = 80\,\text{nm}$.

II. Derivation of Second-order Conic Constraint

Define $f := (\gamma_i^{t+1}+1)^2$ and $g := (\gamma_i^{t+1}-1)^2 + (2z_{i,N_I}^{t+1})^2$. Then

$$f - g = 4\gamma_i^{t+1} - 4(z_{i,N_I}^{t+1})^2 \geqslant 0, \tag{II-1}$$

where the inequality holds because $\gamma_i^{t+1} \geqslant (z_{i,N_I}^{t+1})^2$. Rearrangement of (II-1) yields

$$(\gamma_i^{t+1}+1)^2 \geqslant (\gamma_i^{t+1}-1)^2 + (2z_{i,N_I}^{t+1})^2, \tag{II-2}$$

which is equivalent to the standard second-order conic constraint

$$\left\|\gamma_i^{t+1}+1\right\|_2^2 \geqslant \left\|[\gamma_i^{t+1}-1,\ 2z_{i,N_I}^{t+1}]^{\mathrm{T}}\right\|_2^2. \tag{II-3}$$

III. Battery Cell Parameter Values

For numerical case studies presented in Section III of the main paper, each EV is equipped with 21700-type battery cells with the capacity of $80\,\text{kWh}$. Each EV battery pack has 96 cells in series and 46 cells in parallel (96S46P), with a total of 4416 cells. Each battery cell has capacity $0.005\,\text{kAh}$, nominal voltage $v_{\text{flat},i} = 3.65\,\text{V}$ with operating voltage ranging from $2.5\,\text{V}$ to $4.2\,\text{V}$, and maximum C-rate of 2.5 to avoid excessively sharp charge-discharge cycling. For a battery cell, $\overline{p}_i \approx 3.65 \cdot 0.005 \cdot 2.5 \approx 0.046\,\text{kWh}$. The ambient temperature is assumed to be 28°C. Other parameters related to electrochemical dynamics are given in Table I.

IV. Linear Battery Aging Cost Formulation

In [4], the linear battery degradation cost F_i^t is defined for each charging and discharging cycle at time t until the required state of charge (SoC) in the last time period $t = N_t$, i.e., $S_i^{N_t} = \overline{S}$, yielding

$$F_i^t = C_i \frac{\kappa_i}{100}\left(-\frac{1}{\eta_v} p_{d,i}^t \theta t + \overline{S} - S_i^0\right) \tag{IV-4}$$

where κ_i denotes the slope of the linear approximation of the EV i's battery life as a function of cycles, C_i represents the purchase cost of the EV i's battery divided by its useful capacity [\$/Ah], and S_i^0 is the initial SOC value.

V. Comparison with Nonlinear Battery Aging Cost Formulation

In [5], the nonlinear battery degradation cost G_i^t is obtained from experimental data as an approximation with respect to depth of discharge (DoD) $1 - S_i^t$ and cell current I_i^t (denoted in C-rate). We have

$$G_i^t = \frac{1}{f_c(I_i^t)\cdot f_d(S_i^t)}, \tag{V-5}$$

where f_c and f_d represent battery life loss due to DoDs and cell currents, respectively, and they are given by

$$f_d = \begin{cases} 4000, & \text{if } S_i^t > 0.95, \\ 946.1\cdot(1-S_i^t)^{-1.079}, & \text{if } S_i^t \leqslant 0.95, \end{cases} \tag{V-6a}$$

$$f_c = \begin{cases} 4, & \text{if } I_i^t < 0.2, \\ 1.041\cdot(I_i^t)^{-0.445}, & \text{if } 0.2 \leqslant I_i^t \leqslant 2.5. \end{cases} \tag{V-6b}$$

Substitution of the above in (V-5) then yields

$$G_i^t = \begin{cases} 0.6\cdot 10^{-4}, & \text{if } S_i^t > 0.95,\ I_i^t < 0.2, \\ 0.2\cdot 10^{-3}\cdot(I_i^t)^{0.445}, & \text{if } S_i^t > 0.95,\ 0.2 \leqslant I_i^t \leqslant 2.5, \\ 0.2\cdot 10^{-3}\cdot(1-S_i^t)^{1.079}, & \text{if } S_i^t \leqslant 0.95,\ I_i^t < 0.2, \\ 10^{-3}\cdot(1-S_i^t)^{1.079}\cdot(I_i^t)^{0.445}, & \text{if } S_i^t \leqslant 0.95,\ 0.2 \leqslant I_i^t \leqslant 2.5. \end{cases} \tag{V-7a}$$

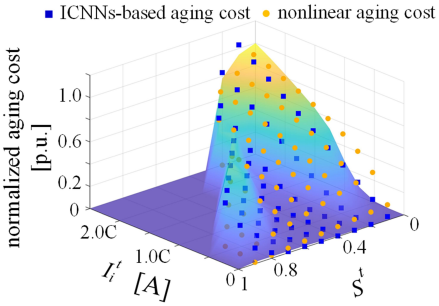

Fig. 2. Comparison between nonlinear and ICNNs-based degradation costs.

We compare the electrochemical degradation costs between the nonlinear method [5] and the ICNNs-based formulation (2b)–(2d) under a random set of 66 SoC values. We normalize the electrochemical degradation costs in a continuous range $[0, 1]$ and present their solutions on the normalized PDE-based degradation surface $\Delta\theta_1^{t+1}$ in Fig. 2. Among data points plotted in Fig. 2, 84.8% of markers have less than 1% error for the ICNNs-based compared with 19.7% for

TABLE I
PARAMETERS FOR ELECTROCHEMICAL KINETICS

Parameter	Negative electrode	Separator	Positive electrode
electrode plate area [m^2]	0.163	0.163	0.163
electrode thickness [m]	$78 \cdot 10^{-6}$	$20 \cdot 10^{-6}$	$45 \cdot 10^{-6}$
Li^+ diffusion coefficient [m^2/s]	$3.9 \cdot 10^{-5}$	-	$1.8 \cdot 10^{-8}$
active electrode volume fraction [%]	0.6	-	0.6
electrolyte phase volume fraction [%]	0.3	-	0.3
max solid phase concentration [mol/m^3]	31507	-	49000
particle radius [m]	$6 \cdot 10^{-6}$	-	$5 \cdot 10^{-6}$
reaction rate efficiency [A/m^2]	$9.77 \cdot 10^{-2}$	-	$1.19 \cdot 10^{-2}$
exchange current density of side reaction [A/m^2]	10	-	10
initial electrolyte concentration [mol/m^3]	$1.25 \cdot 10^4$	$1.25 \cdot 10^4$	$1.25 \cdot 10^4$
Binder volume fraction [%]	0.1	-	0.1
Separator volume fraction [%]	-	0.4	-
Thickness of current collectors [m]	$10 \cdot 10^{-6}$	-	$10 \cdot 10^{-6}$

the nonlinear degradation cost formulation. Furthermore, the ICNNs-based electrochemical degradation cost method has less than 2% error across the domain, and is thus accurate for the optimal V2G dispatch.